Life Sciences 232 (2019) 116639

Contents lists available at ScienceDirect

Life Sciences

journal homepage: www.elsevier.com/locate/lifescie

SIRT2 functions in aging, autophagy, and apoptosis in post-maturation bovine oocytes

Dejun Xu[a], Xiaohan Jiang[a], Huanshan He[a], Dingbang Liu[a], Li Yang[a], Huali Chen[a], Lin Wu[a], Guoxia Geng[b], Qingwang Li[a,*]

[a] College of Animal Science and Technology, Northwest A&F University, Yangling 712100, China
[b] College of Veterinary Medicine, Northwest A&F University, Yangling 712100, China

ARTICLE INFO

Keywords:
SIRT2
oocyte
aging
autophagy
apoptosis

ABSTRACT

Aims: Sirtuins have been implicated in the aging process, however, the functions of SIRT2 in post-maturation aging of oocytes are not fully understood. The purpose of the present investigation was to assess the roles of SIRT2 in aged oocytes and mechanisms involved.

Main methods: The fresh MII oocytes were aging in vitro, and treated with SIRT2 inhibitor (SirReal2), autophagy activator (Rapamycin), and autophagy inhibitor (3-Ma) for 24 h, respectively. Oocyte activation, cytoplasmic fragmentation, and spindle defects, mitochondrial distribution, ROS levels, ATP production, mitochondrial membrane potential, and early apoptosis were investigated. Western blotting was performed to determine LC3-II accumulation, SQSTM1 degradation, and caspase-3 activity.

Key findings: SIRT2 expression gradually decreased in a time-dependent manner during oocyte aging. Treatment with SirReal2 significantly increased the rates of oocyte activation, cytoplasmic fragmentation, and spindle defects. In particular, the high ROS levels, abnormal mitochondrial distribution, low ATP production, and lost ΔΨm were observed in SirReal2-exposed oocytes. Further analysis revealed that LC3-II accumulation and SQSTM1 degradation were induced by SIRT2 inhibition. By performing early apoptosis analysis showed that oocyte aging was accompanied with cellular apoptosis, and SIRT2 inhibition increased apoptosis rates of aged oocytes. Importantly, upregulating autophagy with Rapamycin could mimic the effects of SIRT2 inhibition on apoptosis by increasing caspase-3 activation, whereas downregulating autophagy with 3-MA could abolish those effects by blocking caspase-3 activation.

Significance: Our results suggest that SIRT2 inactivation is a key mechanism underlying of cellular aging, and SIRT2 inhibition contributes to autophagy-dependent cellular apoptosis in post-maturation oocytes.

1. Introduction

Mammalian oocytes are arrested at meiotic metaphase (MII) stage after maturation in vivo or vitro. If no fertilization or artificial activation occurs for a prolonged period, MII oocyte will undergo a time-dependent process of aging, referred to as post-maturation aging [1,2], which results in abnormal spindle morphology [3], mitochondrial dysfunction [4], elevated reactive oxygen species (ROS) levels [1]. The aging-induced impairment for oocytes has marked detrimental effects on fertilization and embryo development [5], even causes oocyte apoptosis [6]. However, mechanisms for post-maturation oocyte aging are still largely unknown.

There are seven Sirtuin family members in mammals that are divided into 4 classes: class I, including SIRT1, SIRT2, and SIRT3; class II, SIRT4; class III, SIRT5; and class IV, SIRT6 and SIRT7 [7,8]. Recently, the role of Sirtuins in the regulation of female reproductive functions has emerged, especially as regards the importance that Sirtuins can have in modulating reproductive aging. SIRT1 involves in the inflammatory response of bovine embryos [9], and decides the quality of aged pig oocytes [10]. SIRT3 deficient has been associated with a lower active deacetylated glutamate dehydrogenase (GDH) form, which alters the metabolism of follicle cells during aging [11]. SIRT4 overexpression causes metabolic dysfunction in oocytes, whereas SIRT4 deletion alleviates the deficient phenotypes of oocytes from aged mice [12]. SIRT6

Abbreviations: MII, Meiotic metaphase; ROS, Reactive oxygen species; ATP, Adenosine triphosphate; ΔΨm, Mitochondrial membrane potential; LC3, Autophagy marker light chain 3; SQSTM1, Sequestosome 1; RT-qPCR, Real-time reverse transcriptase-polymerase chain reaction; cDNA, Complementary DNA

* Corresponding author.
E-mail addresses: nwxudejun@sina.com (D. Xu), 2015060124@nwafu.edu.cn (Q. Li).

https://doi.org/10.1016/j.lfs.2019.116639
Received 7 May 2019; Received in revised form 1 July 2019; Accepted 6 July 2019
Available online 08 July 2019

knockout mice show the defects in a premature aging phenotype [13]. SIRT7 knockdown adversely affects oocytes maturation via disrupting redox homeostasis and cytoskeletal organization [14]. To date, SIRT2 has been linked to the regulation of oocyte meiosis via its deacetylation targets [15]. A recent report shows that SIRT2-BubR1 acetylation pathway can ameliorate the defective phenotypes of oocytes from aged mice [16]. These findings emerge that SIRT2 may mediate post-maturation aging of oocytes; however, the potential functions for SIRT2 on this topic have not been reported.

Autophagy is a highly conserved protein catabolic process by which cytoplasmic contents or organelles are delivered to the lysosome for digestion within a double-membrane autophagosome [17]. Autophagy has been found to be implicated in development of mouse embryos [18] and bovine embryos [19], maturation of porcine oocyte [20]. Autophagy is recognized as an important regulatory mechanism for cell apoptosis, special in unfavorable growth conditions [21]. Escobar-Sánchez et al. [22] demonstrated that apoptosis and autophagy markers are present in all phases of the estrous cycle contained dying oocyte, suggesting that there is a close relationship between apoptosis and autophagy in oocytes. Interestingly, the recent studies show that SIRT2 knockdown increases basal autophagy in multiple cells [23,24]. Furthermore, autophagy is one of the hallmarks of aging, which is observed in post maturation aging of mouse oocytes [25]. These findings hint that a redundancy of function might exist between SIRT2 and autophagy in apoptosis of aged oocytes.

The aim of this study was to investigate SIRT2 functions in aging of oocyte and mechanisms involved. Based on these investigations, we revealed that SIRT2 inactivation aggravates oocyte aging by increasing the ROS levels, mitochondrial dysfunction, spindle defects, autophagy levels. In particular, for the first time, we found that SIRT2 inhibition induced apoptosis by upregulating autophagy during post-maturation oocyte aging.

2. Materials and methods

2.1. Antibodies and chemicals

Rabbit polyclonal anti-SIRT2 (Cat#: 19655-1-AP), mouse monoclonal anti-α-tubulin (Cat#: 66031-1-Ig), and rabbit polyclonal anti-SQSTM1 (Cat#: 18420-1-AP) antibodies were purchased from Proteintech Group Inc. (Wuhan, China). Rabbit polyclonal anti-LC3 (Cat#: 3868) antibody was purchased from cell signaling technology (Danvers, MA, USA). Rabbit polyclonal anti-cleaved-caspase-3(Cat#: ab49822), rabbit monoclonal anti-pro-caspase-3(Cat#: ab 32150), and rabbit monoclonal anti-GAPDH (Cat#: ab181603) antibodies were purchased from Abcam (Cambridge, UK). SirReal2 (Cat#: S7845), Rapamycin (Cat#: S1039), and 3-Methyladenine (3-MA) (Cat#: S2767) were purchased from Selleck chemicals (Houston, TX, USA). Unless otherwise indicated, the other chemicals were purchased from Sigma-Aldrich (St. Louis, MO, USA).

2.2. In vitro maturation and treatment

Bovine ovaries were collected from a local abattoir (Shaanxi, China), and transported to the laboratory within 8 h in phosphate-buffered saline (PBS) containing penicillin (100 IU/mL) and streptomycin (100 mg/mL) at 27–30 °C. The cumulus-oocyte complexes (COCs) with three or more layers of cumulus cells were chosen for in vitro maturation (IVM). After washing three times, approximately 50 COCs was cultured for 24 h in 750 μL of IVM medium at 38.5 °C in 5% CO_2. The IVM medium was TCM-199, supplemented with 10% (*v*/v) fetal bovine serum (FBS), 1% (v/v) ITS (Contains 1.0 mg/mL recombinant human insulin, 0.55 mg/mL human transferrin, and 0.5 μg/mL sodium selenite at the 100 x concentration), 0.1 IU/mL human menopausal gonadotropin (HMG), 0.2 mM sodium pyruvate, 10 ng/mL epidermal growth factor, 0.2 IU/mL follicle-stimulating hormone (Ningbo Second Hormone Factory, Ningbo, China), 2 μg/mL 17β-estradiol, 100 IU/mL penicillin, and 100 mg/mL streptomycin. After IVM, cumulus cells were removed by hyaluronidase. Only oocytes with first polar bodies were used for the experiments. To generate in vitro-aged oocytes, the fresh MII oocytes were cultured in IVM medium, and covered with mineral oil at 38.5 °C in 5% CO_2 for 12, 24, 48 h, with 70% IVM medium being replaced every 12 h, respectively. According to our previously report [26], the optimal concentration of 5 μM SirReal2 was used in this study, whereas 10 nM Rapamycin, and 5 mM 3-MA were obtained from previously published studies on post-maturation oocyte aging [25]. To down or up regulate the activities of autophagy and SIRT2, the fresh MII oocytes were incubated in IVM medium supplement with SirReal2 (5 μM), Rapamycin (10 nM), 3-MA (5 μM) for 24 h, respectively. The control groups were treated with DMSO.

2.3. Activation of oocytes

According to previous studies [27,28], ethanol stimulus was used to evaluate oocytes activation. For ethanol activation, the fresh MII or aged oocytes were first treated with 5% (v/v) ethanol in IVM medium for 5 min at 38.5 °C. After washing three times, oocytes were incubated for 6 h in IVM medium containing 2 mM 6-dimethylamino purine (6-DMAP) at 38.5 °C in 5% CO_2. Then, the ethanol-activated oocytes were cultured for 6 h. At the end of the activation culture, oocytes were observed with inverted microscope for activation, and stained with DAPI to show female pronucleus formation. As previous study described [27,28], only those oocytes that had one or two pronuclei, or two cells each having a nucleus, were considered activated.

2.4. Assessment of oocyte fragmentation

As previously described [27,29], oocytes with more than two asymmetric cells were considered cytoplasmic fragmentation, whereas oocytes with a clear moderately granulate cytoplasm and an intact first polar body were un-fragmented. Oocytes were observed for morphological feature using a phase contrast microscope (Nikon, JP), and percentages of cytoplasmic fragmentation were quantified in fresh, 24 h aged, SirReal2-exposed 24 h aged, 48 h aged, and SirReal2-exposedb 48 h aged oocytes.

2.5. Determination of intracellular ROS

The fluorescent dye 2′,7′-dichlorodihydrofluorescein diacetate (DCFH-DA; Beyotime, China) was used to evaluate intracellular ROS. Briefly, oocytes were incubated for 30 min at 38.5 °C in M199 supplemented with 10 μM DCFH-DA in the dark. After incubation, oocytes were washed with M199 contained 0.1% (w/w) bovine serum albumin (BSA) for removing redundant DCFH-DA, and then the green fluorescence was observed using a fluorescence microscope (Nikon, Japan) with 460 nm UV filters. The fluorescence intensities of oocytes were analyzed by Image-Pro Plus 6.0 software (Media Cybernetics, USA).

2.6. Evaluation of mitochondrial distribution

For mitochondrial staining, oocytes were incubated in M199 containing 100 nM Mito-Tracker Green (Beyotime, China) in the dark at 38.5 °C for 30 min. After washing with M199 contained 0.1% bovine serum albumin (BSA), oocytes were observed with a confocal microscope (Leica, Solms, Germany), and recorded according to a previously described method [30,31]. The normal mitochondrial distribution presented homogeneous mitochondrial that mitochondria are distributed throughout the cytoplasm. Whereas, no mitochondrial signals are observed in some areas (such as in the central and/or peripheral cytoplasm) of the cytoplasm, or/and mitochondria distribution is large, heterogeneous clump distribution (clustering distribution); indicating abnormal mitochondrial distribution. Then, percentages of normal

mitochondrial distribution were quantified in oocytes.

2.7. Determination of intracellular ATP and ΔΨm

ATP fluorometric assay kit (Sigma, USA) was used to evaluate ATP concentration of oocytes. Briefly, a pool of 100 denuded oocytes was lysed with 20 μL of cell lysis reagent. According to kit's instructions, 50 μL of the appropriate reaction mix (containing 45.8 μL of ATP assay buffer, 0.2 μL of ATP probe, 2 μL of ATP converter, 2 μL of developer mix) were added to 20 μL of sample, and the standard solutions (0, 1.0, 2.5, 5.0, 7.5, and 10 pM of ATP) in the 96-well plates, respectively. After incubating at room temperature for 30 min, luminescence intensity was immediately measured using a luminometer (BioTek, USA). A six-point standard curve (0, 1.0, 2.5, 5.0, 7.5, and 10 pM of ATP) was obtained for each series of analyses. Finally, the ATP concentration of the samples was calculated using the formula derived from the standard curve.

The JC-1 assay kit (Beyotime, China) was used to evaluate mitochondrial membrane potential (ΔΨm). According to the manufacturer's instructions, oocytes were incubated in working solution containing 10 μM JC-1 at 38.5 °C for 30 min in the dark. The stained oocytes were washed three times with JC-1 buffer solution, and imaged immediately in green and blue fluorescence channels using a laser scanning microscope (Leica, Solms, Germany). The red and green fluorescence intensities were analyzed by Image-Pro Plus 6.0 software, and ΔΨm was calculated as the ratio of red to green fluorescent pixels.

2.8. Annexin-V staining

Annexin V-fluorescein isothiocyanate (FITC) staining reagent (Vazyme, China) was used for detecting early apoptosis of oocytes. According to manufacturer's instructions, the washed oocytes were incubated in 90 μL of blinding buffer contained 10 μL of Annexin V-FITC for 10 min at room temperature in the dark. Then the stained oocytes were transferred to 4% paraformaldehyde for fixation for 1 h at room temperature in the dark after washed in PBS containing 0.1% (*v*/v) Polyvinyl alcohol (PVA). After fixation and washing, the DNA of oocytes were stained using 4,6-diamidino-2-phenylindole (DAPI, Beyotime). The oocytes were mounted, and the fluorescent signals of green and blue were observed using a fluorescence microscope with 492–520 nm and 420–480 nm filters, respectively.

2.9. Immunofluorescence staining

Immunofluorescence assay was carried out to visualize spindles. Denuded oocytes were washed in PBS containing 0.1% (v/v) PVA three times, then fixed in 4% paraformaldehyde in PBS for 30 min at room temperature. After washing three times in PBS-PVA solution, oocytes were permeabilized for 60 min at room temperature in PBS containing 0.5% (v/v) Triton X-100. Then, the permeabilized oocytes were blocked for 1 h at room temperature with QuickBlock™ blocking buffer (Beyotime, China), and incubated with anti-α-tubulin monoclonal antibodies (1:50) at 4 °C overnight. After washing three times, oocytes were incubated for 1.5 h at room temperature in the dark with Alexa Fluor 488-labeled goat anti-rabbit IgG (1:200). After chromatin staining with DAPI, the stained oocytes were mounted and observed with Leica confocal microscope (Leica, Germany). Fluorescence was detected with 492–520 nm (Alexa Fluor 488), 420–480 nm (DAPI) filters, respectively, and the captured signals of spindle and chromosome were recorded as green, blue, respectively by LAS X software.

2.10. Quantitative real-time PCR

Total RNA of 50 oocytes was extracted with 6 μL of lysis buffer (5 mM dithiothreitol, 2IU/μL RNase inhibitor, 1% NP-40). Then, the first-strand complementary DNA (cDNA) was obtained using a RT reagent kit with genomic DNA Eraser (Takara, Kusatsu, JP). The cDNA of *Sirtuins* was performed quantitative real-time PCR using CFX96TM Real-Time PCR (Bio-Rad, Hercules, CA, USA) with the SYBR Premix Ex TaqII (2×) Reagent Kit (Takara, JP). The thermal cycling parameters for real-time PCR were performed in our previously described protocol [32]. The bovine-specific primers for *Sirtuins* were listed in Table 1. Relative gene expression was calculated by the $2^{-\Delta\Delta Ct}$ method.

Table 1
Sequences for primers used in quantitative real-time RT-PCR.

Gene name	Primer sequences (5′–3′)	GenBank accession No.
SIRT1	F:GGAGCAGATTAGTAAACGCCT R:CTTTCATCCTCCATGGGTTC	NM_001192980
SIRT2	F:CAACCTGGAGAAATACCGTCTT R:CAGTCCTTTTTCCTTCAGCAG	NM_001113531.1
SIRT3	F:GCATGGCGTTGTTTCCTCGT R:TGTCACTTGAGGCACCAGCA	NM_001206669.1
SIRT4	F:CCCCGCTTCCTCTATCTGA R:GGGCTCTTTCTTCTGCCTAAT	NM_001075785.1
SIRT5	F:ACTTCCTCCGTGGTCTATCC R:GACTTTCCAGTATTTGGCTCAC	NM_001034295.2
SIRT6	F:GCGGTCTACCCGAGGTCTTC R:ACACCACACTGGAGGACTGC	NM_001098084.1
SIRT7	F:AGCCTCTATCCCAGATTACCG R:ACACCCGCACATATTCCCTA	NM_001075217.1
GAPDH	F:CACCCTCAAGATTGTCAGCA R:GGTCATAAGTCCCTCCACGA	NM_001034034

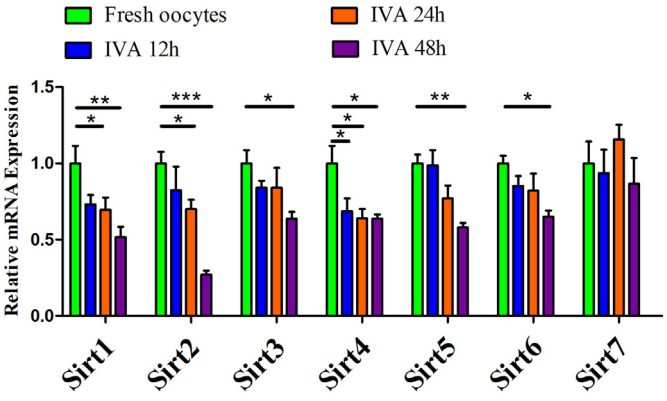

Fig. 1. The mRNA levels of *Sirtuins* were gradually decreased during oocytes aging. The MII oocytes were aging for 12 h, 24 h, and 48 h in vitro. The expression of *Sirt1*, *Sirt2*, *Sirt3*, *Sirt4*, *Sirt5*, *Sirt6*, and *Sirt7* mRNA in fresh and aged oocytes was evaluated by real time RT-PCR analysis. The mRNA level of the control groups was arbitrarily set at 1.0, and that of the treatment groups was estimated relative to the control value. IVA, in vitro aging. Data are expressed as the mean ± SEM from three independent experiments. * $p < 0.05$, ** $p < 0.01$, ***$p < 0.001$, comparing the indicated groups.

2.11. Western blot analysis

A pool of 50 denuded oocytes of each group was lysed in 20 μL of cold RIPA buffer (Beyotime, China), containing 50 mM Tris pH 7.4 , 150 mM NaCl , 1% Triton X-100 , 1% sodium deoxycholate , 0.1% SDS, 1 mM PMSF. The denatured proteins were separated by 15% SDS-PAGE gel, and transferred onto 0.2 μm PVDF membranes (Beyotime, China) with transfer buffer (39 mM glycine, 48 mM Tris, 1% SDS, 20% methanol, pH 8.3). After blocking with TBST (20 mM Tris-HCl, 150 mM NaCl, 0.05% Tween 20), containing 5% (*w*/v) non-fat dry milk, the membranes were incubated overnight at 4 °C with primary antibodies (anti-LC3, 1:500; anti-SQSTM1, 1:500; anti-SIRT2, 1: 1000; anti-procaspase-3, 1: 500; anti-cleaved-caspase-3, 1: 500; anti-GAPDH, 1:10,000), respectively. After washing, the membranes were incubated for 1 h at room temperature with HRP-conjugated goat Anti-rabbit

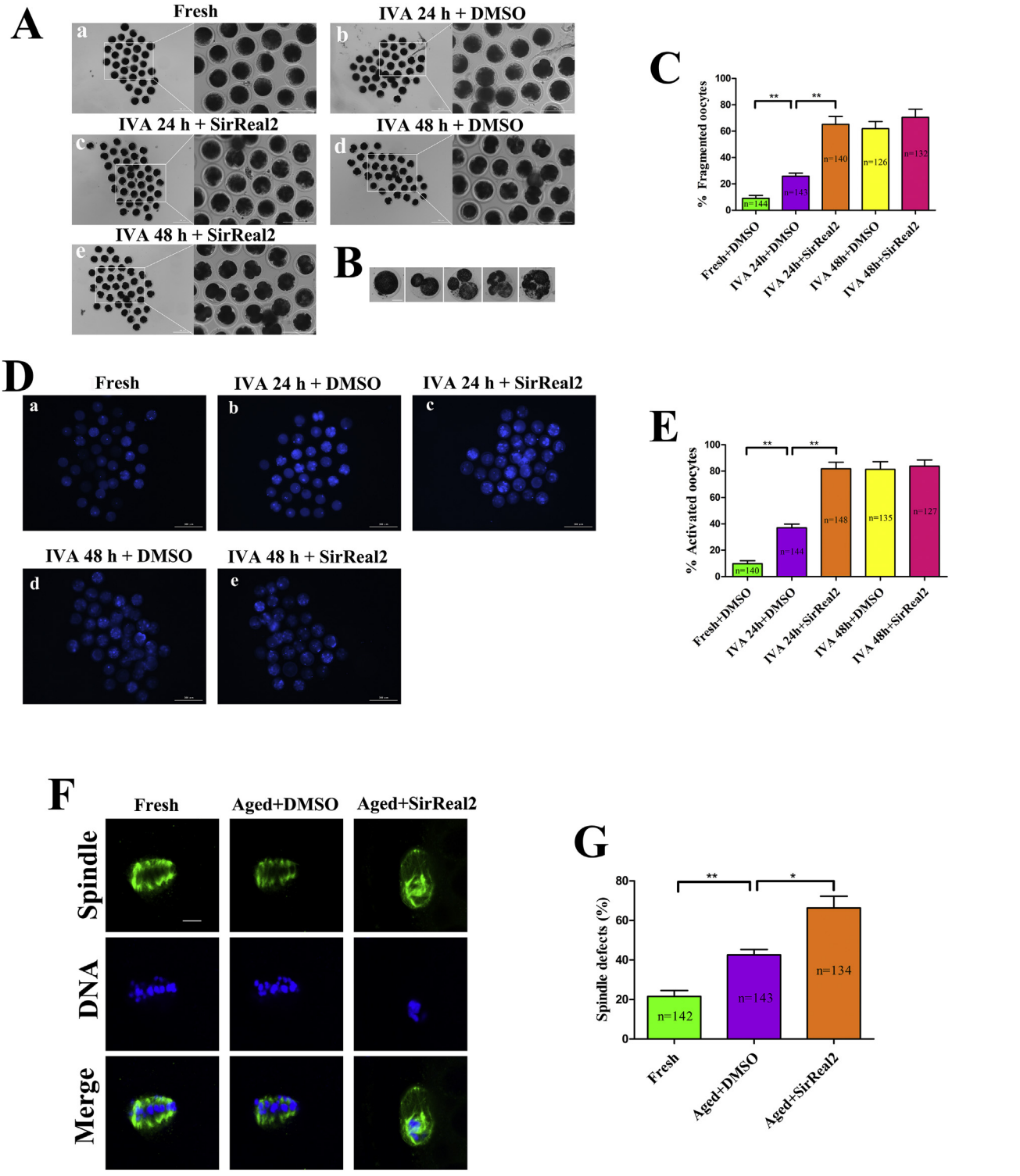

(caption on next page)

IgG(H + L) (1:5000; Sungene Biotech, China). Then the membranes were exposed to X-ray film with ECL Plus (Millipore, Burlington, MA, USA), and band intensities were quantified with Quantity One software (v. 4.52; Bio-Rad Laboratories).

2.12. Statistical analysis

All experiments were repeated at least three times unless specified otherwise. Data were shown as mean ± standard error of the mean (SEM). The differences between treatment groups were calculated with the student's *t*-test using SPSS 20.0 statistical software (SPSS, Chicago, IL, USA). A p value < 0.05 was considered as a statistically significant difference.

Fig. 2. SIRT2 inhibition accelerated oocyte aging. (A) Representative images of oocyte morphology in fresh (a), 24 h aged (b), SirReal2-exposed 24 h aged (c), 48 h aged (d), and SirReal2-exposed 48 h aged (e) oocytes. Scale bar, 300 μm or 200 μm. (B) Representative images of fragmentation of oocytes. Photograph (a) shows un-fragmented oocyte with a clear moderately granulate cytoplasm and an intact first polar body. Photographs (b–e) show fragmented oocytes with more than two asymmetric cells. Scale bars, 100 μm. (C) Percentages of cytoplasmic fragmentation in fresh (n = 144), 24 h aged (n = 143), SirReal2-exposed 24 h aged (n = 140), 48 h aged (n = 126), and SirReal2-exposed 48 h aged (n = 132) oocytes were shown. (D) Representative images of oocyte activation in fresh (a), 24 h aged (b), SirReal2-exposed 24 h aged (c), 48 h aged (d), and SirReal2-exposed 48 h aged (e) oocytes. Oocytes were stained with DAPI to show female pronucleus formation. Scale bar, 300 μm. (E) Percentages of oocyte activation in fresh (n = 140), 24 h aged (n = 144), SirReal2-exposed 24 h aged (n = 148), 48 h aged (n = 135), and SirReal2-exposed 48 h aged (n = 127) oocytes were shown. (F) Representative images of spindle morphologies and chromosome alignment in fresh (a), 24 h aged (b), and SirReal2-exposed 24 h aged (c) oocytes. Oocytes were stained with α-tubulin antibody (green) to visualize the spindles, and counterstained with DAPI (blue) to visualize DNA. Fresh oocytes presented typical spindle poles and well-aligned NDA at the metaphase plate (a). The microtubules of aged oocytes became gradually lost from the spindle, and DNA misalignment was observed in aged oocytes (b). Spindle defects and DNA misalignment were observed in SirReal2-exposed 24 h aged oocytes (c). Scale bars, 10 μm. (G) Quantification of spindle defects. Oocytes with disorganized spindles and misaligned chromosomes were the result of spindle defects. The percentages of spindle defects in the fresh (n = 142), 24 h aged (n = 143), SirReal2-exposed 24 h aged (n = 134) oocytes were shown. Data are expressed as the mean percentage ± SEM from three independent experiments were analyzed. * $p < 0.05$, ** $p < 0.01$, comparing the indicated groups. (For interpretation of the references to colour in this figure legend, the reader is referred to the web version of this article.)

3. Results

3.1. Expression of Sirtuin family during oocytes aging

To investigate the possible connection between *Sirtuins* and post-maturation aging of bovine oocytes, the mRNA expression levels of *Sirt1–7* were evaluated by RT-qPCR assays. As shown in Fig. 1, the mRNA levels of *Sirtuins* except for *Sirt7* were gradually decreased in a time-dependent manner during oocyte aging. In particular, SIRT1, SIRT2, and SIRT5 mRNA levels in vitro aged 48 h (IVA 48 h) were very significantly lower than in those of fresh oocytes ($p < 0.01$, Fig. 1), suggesting that they were strongly associated with the progression of aging.

3.2. SIRT2 inhibition accelerates oocytes aging

To investigate the function of SIRT2 on post-maturation oocytes aging, MII oocytes were exposed to 5 μM SirReal2 during IVA 24 h. As shown in Fig. 2B, oocytes with a clear moderately granulate cytoplasm, and an intact first polar body, were considered to be un-fragmented, whereas oocytes with more than two asymmetric cells were considered to be fragmented. As expected, the results showed that cytoplasmic fragmentation was significantly induced by treatment with SirReal2 in aged at 24 h, whereas treatment with SirReal2 hardly aggravated cytoplasmic fragmentation in aged at 48 h (Fig. 2 A, C), suggesting that SIRT2 might prevent aging-induced abnormal morphology during the early stage of aging. As shown in Fig. 2D, E, there was approximately 40% of activation rate in aged oocytes, which was significantly higher than that of fresh oocytes. Interestingly, treatment with SirReal2 resulted in a significantly increased of activation rate in aged at 24 h, but not in aged at 48 h (Fig. 2E), indicating that SIRT2 inhibition accelerates oocytes aging. Oocyte aging is usually associated with spindle defects. Therefore, we evaluated the spindle morphology in fresh, aging, and SirReal2-treated oocytes. As shown in Fig. 2F, G, confocal microscopy revealed that fresh MII oocytes displayed a typical barrel-shaped spindle with well-aligned chromosomes on the equatorial plate (with only 21.59 ± 5.15% abnormal spindle). However, the microtubules of aged oocytes became gradually lost from the spindle (Fig. 2F). Furthermore, the percentage of spindle defects of aged oocytes was prominent higher in SirReal2-treated oocytes than that in untreated oocytes (66.32 ± 10.22% VS 42.52 ± 4.79%, Fig. 2G). Taken together, these results indicate that SIRT2 inhibition contributes to post-maturation aging of oocytes.

3.3. SIRT2 inhibition aggravates oxidative stress and mitochondrial dysfunction of aged oocytes

Oxidative stress has been considered a key mechanism underlying cellular aging, so the ROS levels were evaluated in 24 h aged oocytes treated with or without SirReal2. The results showed that the ROS content of aged oocytes was significantly higher than that of fresh oocytes (Fig. 3A, B). Furthermore, the accumulation of ROS in aged oocytes was markedly aggravated by treatment with SirReal2 (Fig. 3A, B). Mitochondria are also an important subcellular target of ROS-induced cellular damage during aging. We next investigated whether SIRT2 inhibition affected mitochondrial dysfunction in aged oocytes. As shown in Fig. 3C, mitochondria were evenly distributed throughout the cytoplasm in fresh oocytes, whereas no mitochondrial signals in some areas of the cytoplasm or/and clustering distribution were observed in SirReal2-exposed aged oocytes. Importantly, the percentage of normal mitochondrial distribution in the aged control group was significantly higher than that of the SirReal2 treatment group (37.45 ± 5.85% VS 17.59 ± 2.22%, Fig. 3D). In the next step, mitochondrial membrane potential (ΔΨm) was stained with the inner membrane potential dye JC-1, and the ratio of red/green fluorescence was analyzed for ΔΨm. Clearly, compared to aged oocytes, fresh oocytes showed the highest ΔΨm (Fig. 3E, F). In addition, a significant decrease of ΔΨm was observed in SirReal2-treated oocytes (Fig. 3E, F), indicating that SIRT2 inhibition results in low ΔΨm in aged oocytes. Furthermore, we measured the ATP levels in fresh, aging, and SirReal2-treated oocytes. Results showed that the ATP content was decrease during oocytes aging, and treatment with SirReal2 in aged oocytes led to a ~50% reduction in ATP content compared to untreated aged oocytes (Fig. 3G), suggesting that SIRT2 inactivation may be a main cause of ATP reduction in aging oocytes. Collectively, these data indicate that SIRT2 inhibition aggravates the progression of oocytes aging by inducing oxidative stress and mitochondrial dysfunction.

3.4. SIRT2 modulates autophagic activity of aged oocytes

Autophagy is one of the hallmarks of cellular aging. We next examined whether SIRT2 affected autophagic activity in aged oocytes. As shown in Fig. 4A, B, the protein abundance of SIRT2 was decreased in a time-dependent manner during oocyte aging, whereas LC3-II/LC3-I ratio did not change significantly until IVA 48 h (Fig. 4 A, C). However, the level of LC3-II was increased significantly from IVA 24 h to IVA 48 h (Fig. 4A, D). SQSTM1, a well-known autophagic substrate, has been shown to be degraded by autophagy, which was also decreased significantly from IVA 24 h to IVA 48 h (Fig. 4A, E). These results showed that the expression level of SIRT2 was closely correlated inversely with autophagic activity during oocytes aging. To further confirm that SIRT2 regulates autophagic activity during aging, the MII oocytes were treated with or without SirReal2, Rapamycin (autophagic activator), and 3-MA (autophagic inhibitor) for 24 h, respectively. Compared to the control group, western blot showed that a significant upregulation of LC3-II/LC3-I ratio was observed in both SirReal2 and Rapamycin treated groups, whereas the LC3-II/LC3-I ratio did not change between the 3-MA-treated and control group (Fig. 4F, G). Treatment with SirReal2 or Rapamycin significantly increased the level of LC3-II, which was decreased by 3-MA. Conversely, 3-MA positively regulated SQSTM1

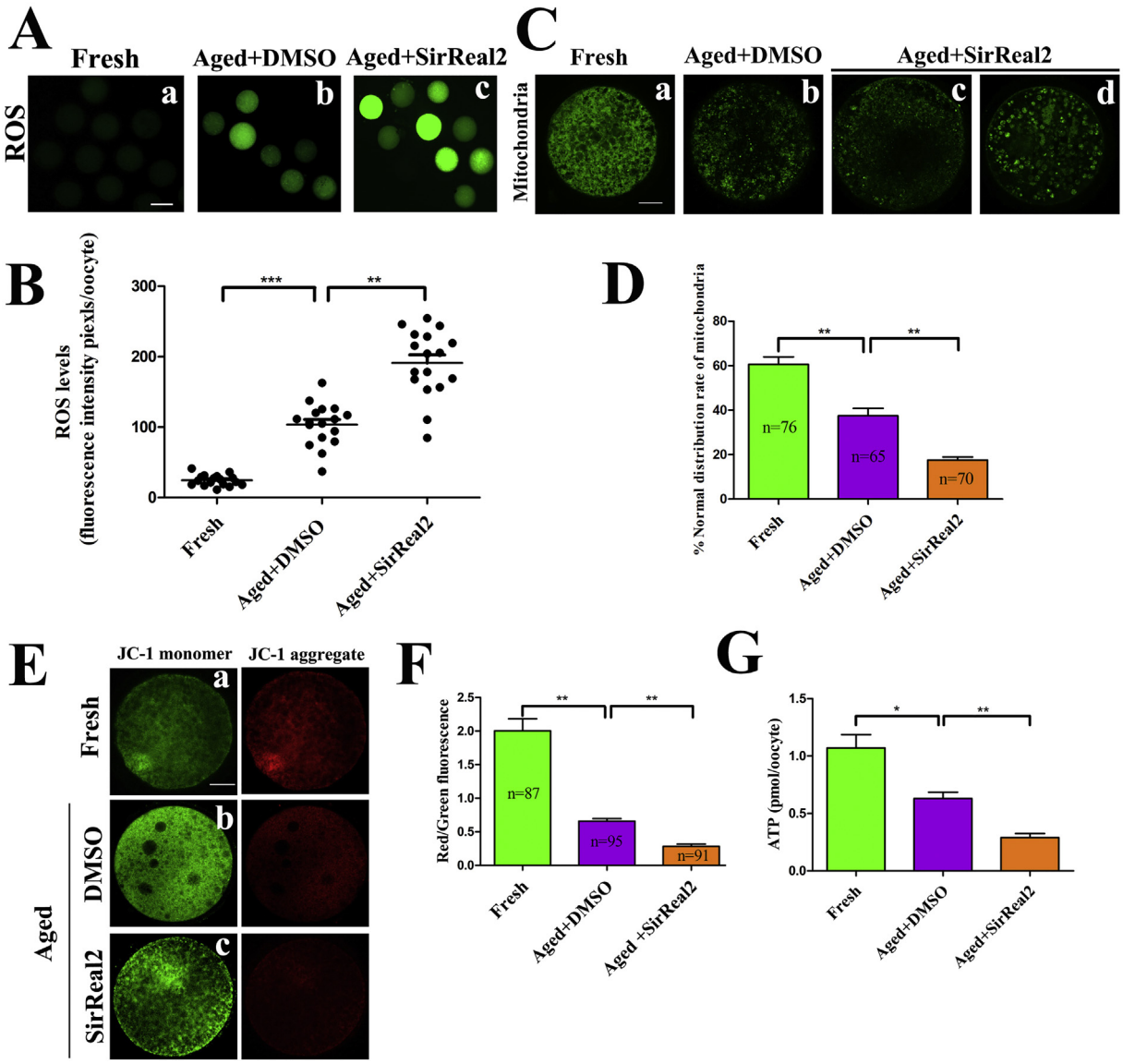

Fig. 3. Effects of SIRT2 on ROS levels and mitochondrial function in 24 h aged oocytes. (A) Representative images of dichloro-dihydro-fluorescein diacetate (DCFH–DA) fluorescence (green) in fresh (a), aged (b), and SirReal2-exposed aged (c) oocytes. Scale bar, 200 μm. (B) Quantification of reactive oxygen species (ROS) fluorescence intensity was analyzed with Image-Pro Plus software. (C) Representative images of mitochondrial distribution patterns visualized with the mito-tracker green in fresh (a), 24 h aged (b), and SirReal2-exposed 24 aged (c-d) oocytes. (a) Normal distribution: mitochondria were distributed throughout the cytoplasm indicated normal distribution. (b–d) Abnormal distribution: (b, c) No mitochondrial signals were observed in some areas of the cytoplasm; (d) clustering distribution. Scale bar, 20 μm. (D) Percentage of normal distribution of mitochondria in the fresh (n = 76), aged (n = 65), and SirReal2-exposed aged (n = 70) oocytes. (E) Representative images of mitochondrial membrane potential (ΔΨm) in the fresh (a), aged (b), and SirReal2-exposed aged (c) oocytes. JC-1 staining was performed to visualize the ΔΨm of oocytes. The red fluorescence (JC-1 aggregates) indicated high membrane potential, whereas the green fluorescence (JC-1 monomers) indicated low membrane potential. Scale bar: 30 μm. (F) Fluorescence pixel ratios (red/green) in the fresh (n = 87), aged (n = 95), and SirReal2-exposed aged (n = 91) oocytes were shown. (G) The ATP content in the fresh, aged, and SirReal2-exposed aged oocytes is shown. Data are expressed as the mean ± SEM from three independent experiments. * $p < 0.05$, ** $p < 0.01$, *** $p < 0.001$, comparing the indicated groups. (For interpretation of the references to colour in this figure legend, the reader is referred to the web version of this article.)

content, whereas treatment with SirReal2 or Rapamycin significantly accelerated the degradation of SQSTM1. Collectively, these results indicated that aging-induced deficiency of SIRT2 enhanced autophagic activity during oocytes aging.

3.5. SIRT2 inhibition promotes apoptosis of aged oocytes via upregulating autophagy

The Annexin V-FITC and ΔΨm assay were carried out to detect the early apoptosis events during oocytes aging. The green fluorescent circle located on the external cellular membrane of the oocyte was defined as Annexin V positive, indicating early apoptosis; whereas only a weak signal would be defined as negative (Fig. 5A). In addition, the decrease of ΔΨm is a hallmark event for early apoptosis. As shown in Fig. 5B, the early apoptosis rate was gradually increased in a time-dependent manner during oocyte aging, suggested that oocyte aging is accompanied by cellular apoptosis. We further studied the mechanism underlying of apoptosis in aged oocytes. As shown in Fig. 5C, D, E, the early apoptosis rate of IVA 24 h oocytes was induced by treatment with SirReal2 or Rapamycin, whereas 3-MA inhibited apoptosis. Importantly, the upregulation effect of SirReal2 on apoptosis was abolished by 3-MA (Fig. 5C, E). These results supported that SIRT2 inhibition induced apoptosis of aged oocytes by increasing autophagic activity. Unexpectedly, the stimulated effect of SirReal2 on activation

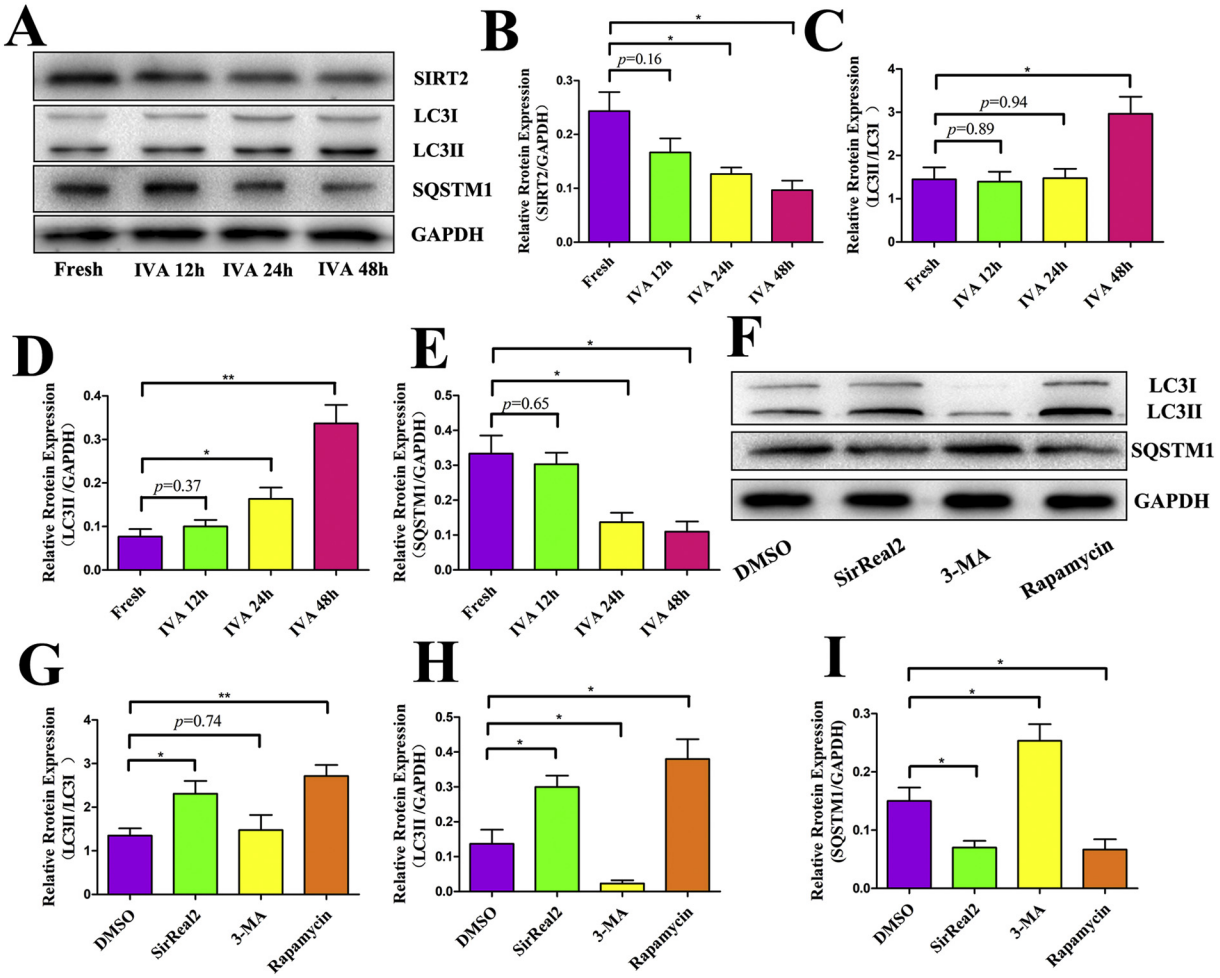

Fig. 4. SIRT2 regulated autophagic activity in aged oocytes. (A) SIRT2 was closely correlated inversely with autophagic activity during oocytes aging. Western blotting for SIRT2, LC3, and SQSTM1 is shown in IVA 12 h, IVA 24 h, and IVA 48 h oocytes. (B-E) The ratios of SIRT2 to GAPDH, LC3-II to LC3-I, LC3-II to GAPDH, and SQSTM1 to GAPDH expression were normalized and the values are shown, respectively. (F) SIRT2 inhibition increased autophagic activity. The MII oocytes were cultured in aging medium supplemented with or without SirReal2 (5 μM), Rapamycin (10 nM), or 3-MA (1 μM) for 24 h. Then, oocytes were harvested for western blotting. (G-I) The ratios of LC3-II to LC3-I, LC3-II to GAPDH, and SQSTM1 to GAPDH expression were normalized and the values are shown, respectively. Data are shown as the means ± SEM of three independent replicates. * $p < 0.05$, ** $p < 0.01$, comparing the indicated groups.

rate did not be changed by Rapamycin or 3-MA, suggesting that SIRT2 did not depend on autophagy mediating oocytes aging (Fig. 5 F). Mechanistically, the cleaved-caspase-3/pro-caspase-3 ratio was increased by SIRT2 inhibition with SirReal2 or upregulating autophagy with Rapamycin, and the ratio was decreased by downregulating autophagy with 3-MA (Fig. 5G, H). Of note, the upregulation effect of SIRT2 inhibition on caspase-3 activity was blocked by downregulating autophagy (Fig. 5G, H). Taken together, these results demonstrated that SIRT2 serves the downregulation function on caspase-3 activity via suppressing basal autophagy, thereby preventing apoptosis in aged oocytes.

4. Discussion

Recently, Sirtuins have emerged as protectors of oocyte against aging in vitro or animal models [10,12,13]. Previous studies have shown that Sirtuins expression is downregulating in aged oocytes [33,34]. Similar to this finding, we found that *Sirt2* mRNA expression was decreased markedly during post-maturation oocytes aging, suggesting that the downregulating of SIRT2 may contribute to aging. This led us to explore how SIRT2 regulates oocytes aging. In this study, SIRT2 inactivation contributed to aging-induced defects by disturbing spindle organization, oxidative stress, and mitochondrial dysfunction. In particular, for the first time, we found that SIRT2 inhibition upregulated caspase-3 activity via increasing autophagic activity, thereby resulting in apoptosis of aged oocytes. Previous studies have shown that SIRT2 appears to a link with aging. For example, SIRT2 overexpression ameliorates maternal age-associated oocyte meiotic defects in a mouse model [16,35]. Whereas our results provided direct evidence for the first time that SIRT2 inhibition resulted in aged phenotypes including cellular fragmentation, spindle defects, elevated ROS accumulation, mitochondrial dysfunction, and upregulating autophagy.

Multiple factors appear to contribute to oocytes aging, whereas one of the most severe challenges that ROS-induced oocytes aging in vitro [1]. We also found that aged oocytes exhibit increased levels of ROS. The decline of antioxidant defences may lead to ROS accumulation, thereby causing oocytes oxidative stress. It well known that SIRT1 protects aged oocytes from oxidative stress by antioxidant defences [10,34]. Compared to SIRT1, the potential roles of SIRT2 on redox homeostasis remain largely unveiled during oocytes aging. Here we found SIRT2 inhibition with SirReal2 aggravated oxidative stress in aged oocytes. Similar to our observations, Zhang et al. [35] found that Sirtuins inhibition by NAM, a pan-inhibitor of Sirtuins, results in a marked increase of ROS levels during in vitro aging. These results suggested that SIRT2 may play important role in redox homeostasis, whereas aging-induced SIRT2 downregulating disturbs the antioxidant

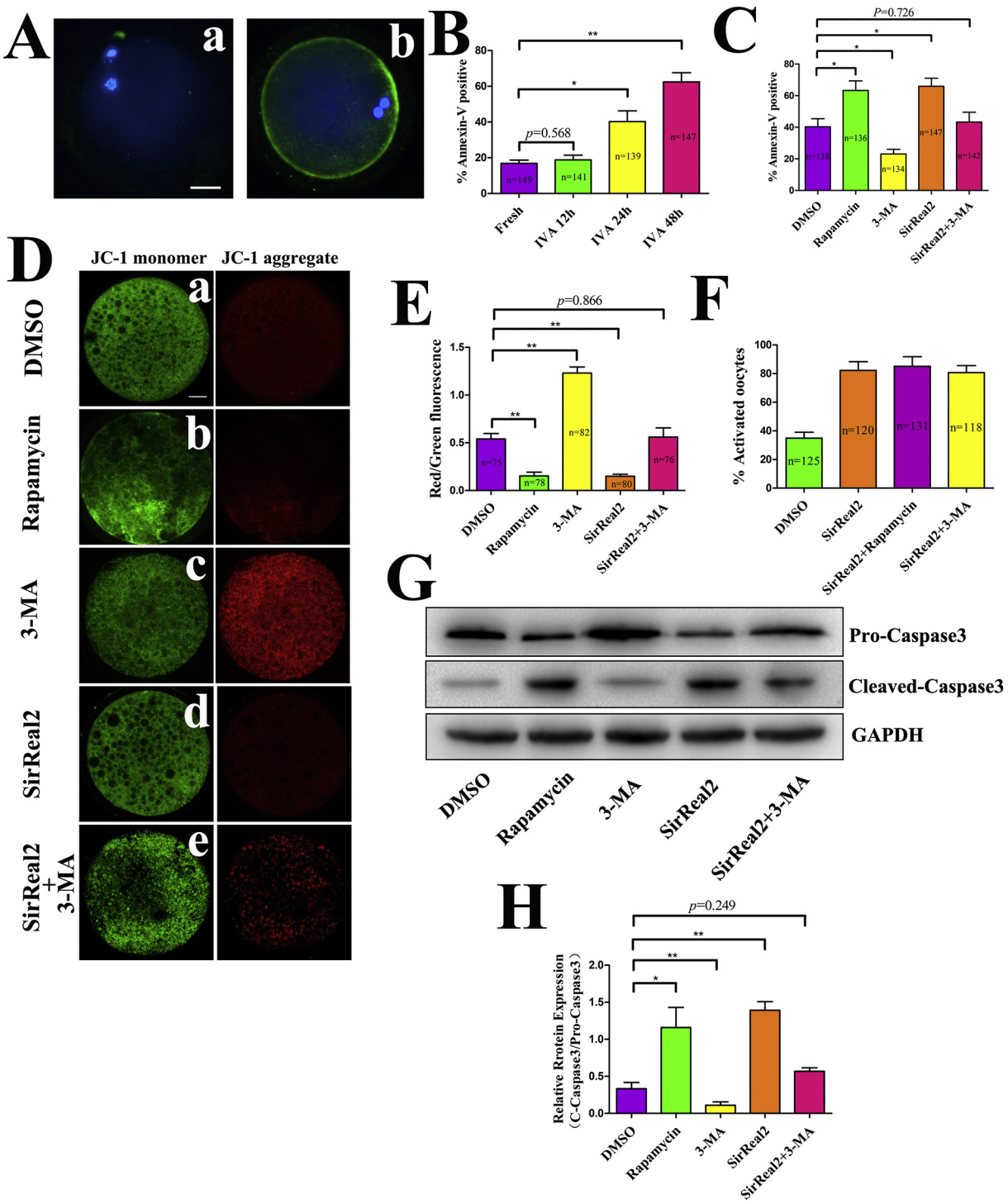

Fig. 5. SIRT2 inhibition induced apoptosis of aged oocytes. (A) Representative images of Annexin-V negative (a) or apoptosis positive (b) in 24 aged oocytes. Scale bar, 50 μm. (B) The ratios of early apoptosis were recorded in fresh (n = 149), 12 h aged (n = 141), 24 h aged (n = 139), and 48 h aged (n = 147) oocytes. (C) The MII oocytes were aged for 24 h in aging medium containing DMSO, Rapamycin (10 nM), 3-MA (1 μM), SirReal2 (5 μM), or SirReal2 (5 μM) + 3-MA (1 μM), respectively. The ratios of early apoptosis were observed in the control (n = 138), and treatment with Rapamycin (n = 136), 3-MA (134), SirReal2 (n = 147), or SirReal2 + 3-MA (n = 142) groups. (D) Representative images of mitochondrial membrane potential in the control (a), treatment with Rapamycin (b), 3-MA (c), SirReal2 (d), and SirReal2 + 3-MA (e) groups in 24 h aged oocytes. Scale bar, 30 μm. (E) Fluorescence pixel ratios (red/green) in the control (n = 75), treatment with Rapamycin (n = 78), 3-MA (n = 82), SirReal2 (n = 80), and SirReal2 + 3-MA (n = 76) groups are shown. (F) The ratios of activated oocytes were shown in 24 h aged oocytes by treatment with DMSO, SirReal2, SirReal2 + Rapamycin, or SirReal2 + 3-MA, respectively. (G) Western blotting for pro-caspase3, cleaved-caspase3, and GAPDH was shown in 24 h-aged oocytes by treatment with DMSO, Rapamycin, SirReal2, and SirReal2 + 3-MA, respectively. (H) The ratio of cleaved-caspase3 to pro-caspase3 expression were normalized and the values are shown. Data are shown as the means ± SEM of three independent replicates. * $p < 0.05$, ** $p < 0.01$, comparing the indicated groups. (For interpretation of the references to colour in this figure legend, the reader is referred to the web version of this article.)

system in aged oocytes.

It is worth noting that mitochondria provide the majority of ATP for oocytes [36]. Moreover, early studies have reported that postovulatory oocyte aging was involved in mitochondrial injury [37]. Compared with SIRT3 and SIRT4, the effect of SIRT2 on mitochondria is not clear, especially in aged oocytes. Therefore, we investigated the functions of SIRT2 on mitochondrial function during oocytes aging. Although SIRT2 is not located in mitochondria, we revealed that SIRT2 inhibition resulted in abnormal mitochondrial distribution, ΔΨm disappearance and ATP production reduction in aged oocytes. Similarly, a recent study reported that mitochondrial dysfunction had been emerged in aged $Sirt2^{-/-}$ mice [38]. These findings supported that SIRT2 may play a key role in maintaining mitochondrial function during oocytes aging.

Recent studies show that autophagy is one of the hallmarks of aging, which involves a decline in the number and functionality of stem cells [39]. Interestingly, we also found that autophagic activity was upregulating during oocytes aging. Then we investigated the mechanism underlying of increased autophagy in aged oocytes. The close relationship between SIRT2 and autophagy has been demonstrated in several prior studies. SIRT2-knockdown increases autophagy through LC3-II accumulation and SQSTM1 degradation in HCT116 cells [23]. In addition, SIRT2-dependent deacetylation induces autophagy through acetylation of FoxO1 in H1299 cells [24]. SIRT2 also interacts with HDAC6 that plays a role in lysosome-autophagosome fusion [40]. These observations are similar to our present results that SIRT2 inhibition with SirReal2 increased autophagic activity through LC3-II accumulation and SQSTM1 degradation in aged oocytes. It had been shown that oocyte aging is accompanied by cellular apoptosis. The dead cells show high levels of autophagy, and ATG5 can directly affect proapoptotic factors to initiate apoptosis pathway [41]. It has been reported that autophagy and apoptosis may be closely connected by common regulators [42]. A recent report has shown that Sirtuins inhibition result in autophagy and apoptosis in porcine preimplantation blastocysts [43]. Similarly, the apoptosis of aged oocytes was induced by inhibition SIRT2 or upregulating autophagy in this study. Importantly, we found that the effect of SIRT2 inhibition on apoptosis was abolished by blocking autophagy. Further studies showed that SIRT2 inhibition contributed to caspase3-dependent oocytes apoptosis by upregulating autophagy. As Chung et al. [44] reported that abnormal induction of autophagic flux promotes apoptotic neuronal cell death via mediating caspase-3 activation. Consistent with our results, previous studies reported that caspase-3 activation was upregulated by autophagy in ovarian nurse cells [45], vascular endothelial cells [46]. Similar to our observations, Lin et al. [25] found that the increased caspase-3 activation of oocytes was accompanied with autophagy in aged at 14 h or 18 h. These evidences support the notion that SIRT2 might mediate apoptosis of aged oocytes via autophagy-induced caspase-3.

5. Conclusions

In summary, our results highlight the important function of SIRT2 in aged oocytes. Our findings may explain, at least in part, how oocytes undergo a time-dependent process of aging. A possible mechanism underlying is that aging-induced downregulating of SIRT2 accelerate aging process by disturbing spindle organization, oxidative stress, and mitochondrial dysfunction, and finally lead to apoptotic cell death though autophagy-induced caspase-3. This study provides insights that SIRT2 activators may offer novel opportunities for delaying post-maturation aging of oocytes.

Declaration of Competing Interest

The authors declare no conflict of interest.

Acknowledgment

We gratefully acknowledge the abattoir unit of QinBao Animal Husbandry Co. for providing the bovine ovarian samples.

Funding

This work was funded by the National Key Technology Support Program (2015BAD03B04) and Ministry of Agriculture transgenic major projects (2018ZX0801013B).

References

[1] T. Lord, R.J. Aitken, Oxidative stress and ageing of the post-ovulatory oocyte, Reproduction 146 (2013) 217–227.
[2] Y.L. Miao, K. Kikuchi, Q.Y. Sun, H. Schatten, Oocyte aging: cellular and molecular changes, developmental potential and reversal possibility, Hum. Reprod. Update 15 (2009) 573–585.
[3] Teng Zhang, Yang Zhou, Li Li, Hong-Hui Wang, Xue-Shan Ma, Wei-Ping Qian, Wei Shen, Heide Schatten, Qing-Yuan Sun, SIRT1, 2, 3 protect mouse oocytes from postovulatory aging, AGING. 8 (2016) 685–696.
[4] E.A. Seidler, K.H. Moley, Metabolic determinants of mitochondrial function in oocytes, Semin. Reprod. Med. 33 (2015) 396–400.
[5] J.J. Tarin, S. Perez-Albala, A. Aguilar, J. Minarro, C. Hermenegildo, A. Cano, Long-term effects of postovulatory aging of mouse oocytes on offspring: a two-generational study, Biol. Reprod. 61 (1999) 1347–1355.
[6] C. Tatone, M.C. Carbone, R. Gallo, S. Delle Monache, M. Di Cola, E. Alesse, F. Amicarelli, Age-associated changes in mouse oocytes during postovulatory in vitro culture: possible role for meiotic kinases and survival factor BCL2, Biol. Reprod. 74 (2006) 395–402.
[7] R.A. Frye, Phylogenetic classification of prokaryotic and eukaryotic Sir2-like proteins, Biochem. Biophys. Res. Commun. 273 (2000) 793–798.
[8] S. Greiss, A. Gartner, Sirtuin/Sir2 phylogeny, evolutionary considerations and structural conservation, Mol. Cells. 28 (2009) 407–415.
[9] I. Khan, S.W. Kim, K.L. Lee, S.H. Song, A. Mesalam, M.M.R. Chowdhury, Z. Uddin, K.H. Park, I.K. Kong, Polydatin improves the developmental competence of bovine embryos in vitro via induction of sirtuin 1 (Sirt1), Reprod. Fertil. Dev. 29 (2017) 2011–2020.
[10] R. Ma, Y. Zhang, L. Zhang, J. Han, R. Rui, Sirt1 protects pig oocyte against in vitro aging, Anim. Sci. J. 86 (2015) 826–832.
[11] L. Pacella-Ince, D.L. Zander-Fox, M. Lan, Mitochondrial SIRT3 and its target glutamate dehydrogenase are altered in follicular cells of women with reduced ovarian reserve or advanced maternal age, Hum. Reprod. 29 (2014) 1490–1499.
[12] J. Zeng, M. Jiang, X. Wu, F. Diao, D. Qiu, X. Hou, H. Wang, L. Li, C. Li, J. Ge, J. Liu, X. Ou, Q. Wang, SIRT4 is essential for metabolic control and meiotic structure during mouse oocyte maturation, Aging Cell 17 (2018) e12789.
[13] C. Xiao, H.S. Kim, T. Lahusen, R.H. Wang, X. Xu, O. Gavrilova, W. Jou, D. Gius, C.X. Deng, SIRT6 deficiency results in severe hypoglycemia by enhancing both basal and insulin-stimulated glucose uptake in mice, J. Biol. Chem. 285 (2010) 36776–36784.
[14] M. Gao, X. Li, Y. He, L. Han, D. Qiu, L. Ling, H. Liu, J. Liu, L. Gu, SIRT7 functions in redox homeostasis and cytoskeletal organization during oocyte maturation, FASEB J. 32 (2018) 6228–6238.
[15] L. Zhang, X. Hou, R. Ma, K. Moley, T. Schedl, Q. Wang, Sirt2 functions in spindle organization and chromosome alignment in mouse oocyte meiosis, FASEB J. 28 (2014) 1435–1445.
[16] D. Qiu, X. Hou, L. Han, X. Li, J. Ge, Q. Wang, Sirt2-BubR1 acetylation pathway mediates the effects of advanced maternal age on oocyte quality, Aging Cell 17 (2018) e12698.
[17] D.J. Klionsky, Autophagy: from phenomenology to molecular understanding in less than a decade, Nat Rev Mol Cell Biol 8 (2007) 931–937.
[18] S. Tsukamoto, A. Kuma, M. Murakami, C. Kishi, A. Yamamoto, N. Mizushima, Autophagy is essential for preimplantation development of mouse embryos, Science 321 (2008) 117–120.
[19] B.S. Song, S.B. Yoon, J.S. Kim, B.W. Sim, Y.H. Kim, J.J. Cha, S.A. Choi, H.K. Min, Y. Lee, J.W. Huh, S.R. Lee, S.H. Kim, D.B. Koo, Y.K. Choo, H.M. Kim, S.U. Kim, K.T. Chang, Induction of autophagy promotes preattachment development of bovine embryos by reducing endoplasmic reticulum stress, Biol. Reprod. 87 (2012) 1–11.
[20] S. Lee, Y. Hiradate, Y. Hoshino, K. Tanemura, E. Sato, Quantitative analysis in LC3-II protein in vitro maturation of porcine oocyte, Zygote 22 (2014) 404–410.
[21] L. Duprez, E. Wirawan, T. Vanden Berghe, P. Vandenabeele, Major cell death pathways at a glance, Microbes Infect. 11 (2009) 1050–1062.
[22] M.L. Escobar-Sánchez, O.M. Echeverría-Martínez, G.H. Vázquez-Nin, Immunohistochemical and ultrastructural visualization of different routes of oocyte elimination in adult rats, Eur. J. Histochem. 56 (2012) 102–110.
[23] Toshiaki Inoue, Yuji Nakayama, Yanze Li, Haruka Matsumori, Haruka Takahashi, Hirotada Kojima, Hideki Wanibuchi, Motonobu Katoh, Mitsuo Oshimura, SIRT2 knockdown increases basal autophagy and prevents postslippage death by abnormally prolonging the mitotic arrest that is induced by microtubule inhibitors, FEBS J. 281 (2014) 2623–2637.
[24] Y. Zhao, J. Yang, W. Liao, X. Liu, H. Zhang, S. Wang, D. Wang, J. Feng, L. Yu,

W.G. Zhu, Cytosolic FoxO1 is essential for the induction of autophagy and tumour suppressor activity, Nat. Cell Biol. 12 (2010) 665–675.
[25] F.H. Lin, W.L. Zhang, H. Li, X.D. Tian, J. Zhang, X. Li, C.Y. Li, J.H. Tan, Role of autophagy in modulating post-maturation aging of mouse oocytes, Cell Death Dis. 9 (2018) e308.
[26] D. Xu, L. Wu, X. Jiang, L. Yang, J. Cheng, H. Chen, R. Hua, G. Geng, L. Yang, Q. Li, SIRT2 inhibition results in meiotic arrest, mitochondrial dysfunction, and disturbance of redox homeostasis during bovine oocyte maturation, Int. J. Mol. Sci. 20 (2019) e1365.
[27] J. Zhu, J. Zhang, H. Li, T.Y. Wang, C.X. Zhang, M.J. Luo, J.H. Tan, Cumulus cells accelerate oocyte aging by releasing soluble Fas ligand in mice, Sci. Rep. 5 (2015) e8683.
[28] Y.L. Miao, X.Y. Liu, T.W. Qiao, D.Q. Miao, M.J. Luo, J.H. Tan, Cumulus cells accelerate aging of mouse oocytes, Biol. Reprod. 73 (2005) 1025–1031.
[29] E. Lim, T. Choi, A phenotypic study of murine oocyte death in vivo, J Reprod Develop. 50 (2004) 179–183.
[30] M. Stojkovic, S.A. Machado, P. Stojkovic, V. Zakhartchenko, P. Hutzler, P.B. Gonçalves, E. Wolf, Mitochondrial distribution an adenosine triphosphate content of bovine oocytes before and after in vitro maturation: correlation with morphological criteria and developmental capacity after in vitro fertilization and culture, Biol. Reprod. 64 (2001) 904–909.
[31] Q. Yang, S. Dai, X. Luo, J. Zhu, F. Li, J. Liu, G. Yao, Y. Sun, Melatonin attenuates postovulatory oocyte dysfunction by regulating SIRT1 expression, Reproduction 156 (2018) 81–92.
[32] D. Xu, H. He, X. Jiang, R. Hua, H. Chen, L. Yang, J. Cheng, J. Duan, Q. Li, SIRT2 plays a novel role on progesterone, estradiol and testosterone synthesis via PPARs/LXR alpha pathways in bovine ovarian granular cells, J. Steroid Biochem. Mol. Biol. 185 (2019) 27–38.
[33] G. Di Emidio, S. Falone, M. Vitti, A.M. D'Alessandro, M. Vento, C. Di Pietro, F. Amicarelli, C. Tatone, SIRT1 signalling protects mouse oocytes against oxidative stress and is deregulated during aging, Hum. Reprod. 29 (2014) 2006–2017.
[34] T. Zhang, Y. Zhou, L. Li, H.H. Wang, X.S. Ma, W.P. Qian, W. Shen, H. Schatten, Q.Y. Sun, SIRT1, 2, 3 protect mouse oocytes from postovulatory aging, Aging 8 (2016) 685–696.
[35] L. Zhang, R. Ma, J. Hu, X. Ding, Y. Xu, Sirtuin inhibition adversely affects porcine oocyte meiosis, PLoS One 10 (2015) e0132941.
[36] Y. Yu, R. Dumollard, A. Rossbach, F.A. Lai, K. Swann, Redistribution of mitochondria leads to bursts of ATP production during spontaneous mouse oocyte maturation, J. Cell. Physiol. 224 (2010) 672–680.
[37] T. Takahashi, H. Igarashi, M. Amita, S. Hara, K. Matsuo, H. Kurachi, Molecular mechanism of poor embryo development in postovulatory aged oocytes: mini review, J. Obstet. Gynaecol. Res. 39 (2013) 1431–1439.
[38] S. Fourcade, L. Morató, J. Parameswaran, M. Ruiz, T. Ruiz-Cortés, M. Jové, A. Naudí, P. Martínez-Redondo, M. Dierssen, Loss of SIRT2 leads to axonal degeneration and locomotor disability associated with redox and energy imbalance, Aging Cell 16 (2017) 1404–1413.
[39] Miren Revuelta, Ander Matheu, Autophagy in stem cell aging, Aging Cell 16 (2017) 912–915.
[40] J.-Y. Lee, H. Koga, Y. Kawaguchi, W. Tang, E. Wong, Y.-S. Gao, U.B. Pandey, S. Kaushik, E. Tresse, J. Lu, J.P. Taylor, A.M. Cuervo, T.-P. Yao, HDAC6 controls autophagosome maturation essential for ubiquitin-selective quality-control autophagy, EMBO J. 29 (2010) 969–980.
[41] Y. Liu, B. Levine, Autosis and autophagic cell death: the dark side of autophagy, Cell Death Differ. 22 (2014) 367–376.
[42] J.M. Gump, A. Thorburn, Autophagy and apoptosis: what is the connection? Trends Cell Biol. 21 (2011) 387–392.
[43] M.G. Kim, D.H. Kim, H.R. Lee, J.S. Lee, S.J. Jin, H.T. Lee, Sirtuin inhibition leads to autophagy and apoptosis in porcine preimplantation blastocysts, Biochem. Biophys. Res. Commun. 488 (2017) 603–608.
[44] Y. Chung, J. Lee, S. Jung, Y. Lee, J.W. Cho, Y.J. Oh, Dysregulated autophagy contributes to caspase-dependent neuronal apoptosis, Cell Death Dis. 9 (2018) e1189.
[45] Y.C.C. Hou, S. Chittaranjan, S.G. Barbosa, K. McCall, S.M. Gorski, Effector caspase Dcp-1 and IAP protein Bruce regulate starvation-induced autophagy during Drosophila melanogaster oogenesis, J. Cell Biol. 182 (2008) 1127–1139.
[46] C. Jiang, L. Jiang, Q. Li, X. Liu, T. Zhang, G. Yang, C. Zhang, N. Wang, X. Sun, L. Jiang, Pyrroloquinoline quinine ameliorates doxorubicin-induced autophagy-dependent apoptosis via lysosomal-mitochondrial axis in vascular endothelial cells, Toxicology 7 (2019) e152238.